Indian Institute of Technology, Kanpur
Department of Aerospace Engineering

AE625: TRANSITION AND TURBULENCE (Spring 2021)

Instructor: Prof. Navrose

TERM PAPER

Boundary Layer

Instabilities and Transition

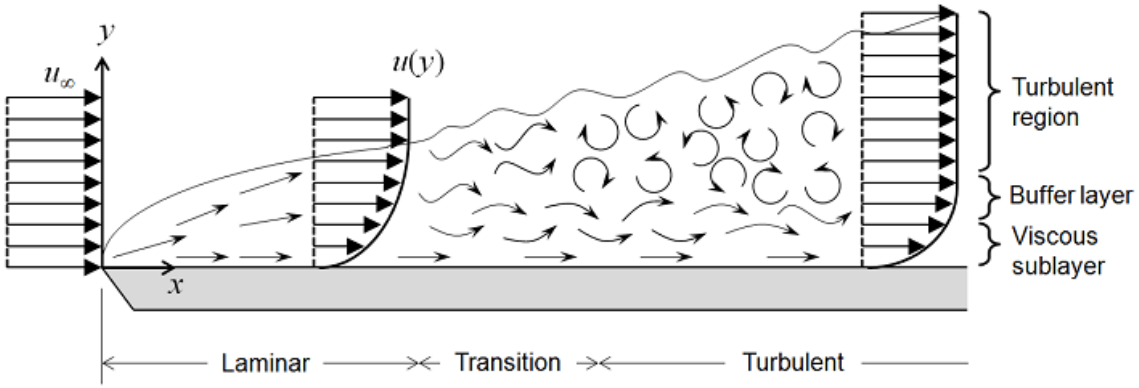

GROUP 2

Abhijeet	**17807015**
Bharat Swami	**170207**
Harish Dechiraju	**17807286**
Pragya Patel	**17807477**

CONTENTS

1. INTRODUCTION

The Navier-Stokes equations represent the motion of viscous fluids mathematically. The stationary solutions to these equations are Laminar flows (no mixing of lateral layers). Disturbances imparted to such flows may develop and affect the flow. Depending on whether the flow is stable or unstable, the disturbances may die out after a while, persist, or even grow to distort the mean flow leading to turbulence. This process of laminar flow becoming a turbulent one is known as *Laminar-turbulent transition*, or simply, *transition*. Instabilities of inviscid flows may arise due to inertial effects (e.g., jet, mixing layers) whereas, for viscous flows, instabilities occur due to the coupling between the inertial, viscous terms and the boundary conditions of the base flow.

Stability

The Navier-Stokes equations can be used to investigate the stability of fluid flows about a base state via perturbation analysis. Such a perturbation analysis mainly involves introducing a small perturbation to the flow and observing the evolution of the disturbance with time and space (temporal, spatial, and spatio-temporal analyses). Suppose for a particular system, the perturbation remains small throughout. In that case, the base state is said to be Lyapunov stable, and if it returns to the base state, the system is Asymptotically stable. Moreover, if the system returns to the base state for any arbitrary perturbation, then the system is globally stable. For infinitesimally small perturbations, we can simplify the Navier-Stokes equations into an eigenvalue problem by linearizing the system about the base state. The eigenvalue formulation of the linearized Navier-Stokes equations for a viscous parallel flow with a two-dimensional perturbation gives the **Orr-Sommerfeld Equation**. The solutions to this equation are the eigenspectra depending on the base flow.

Receptivity

In addition to how a particular perturbation affects the flow, another important one is what kind of perturbations affect the flow the most. The receptivity analysis is a way to analyze the susceptibility of the base flow to various forms of perturbations via Input-Output analysis. This can further answer how a flow may transition into turbulence due to external disturbances (e.g., acoustic disturbances), and how the flow would respond to external forcing (e.g., whether it would amplify the forcing energy). Together with the stability analysis, the response of the eigenvalues obtained earlier can be studied to identify optimal conditions and control the growth of the perturbations.

This report focuses on the stability and receptivity analysis of the **boundary layer over a flat plate**.

2. OVERVIEW

A brief overview of the tasks undertaken during the course are listed below.

1. Solving for the base flow: ***boundary layer over a flat plate***
2. Stability Analysis:
    a. Local linear stability analysis for temporal modes and studying the eigenmodes obtained using the Orr-Sommerfeld equation. For this part, we used the base flow profile from (1) and observed the modes at different streamwise locations.
    b. Global stability analysis of a cubic profile via the Compound Matrix Method.
3. Receptivity Analysis:
    a. Model system: Behaviour of a linear system ODE (simple harmonic oscillator with varying frequency)
    b. Receptivity of boundary layer to wall excitation. For this section, the response to a time harmonic localized disturbance source was considered.
    c. Singular Perturbation problem: We also studied the near field response of this localized excitation to an asymptotic form of the Orr-Sommerfeld equation. (Note: Theoretical approach was used for the receptivity analysis and not for the base flow profiles obtained in (1))

Problem Setup for the base flow calculations

The solution provides a laminar boundary layer on the surface, which can be compared to the Blasius solution as a verification case for SU2. The details of the code can be viewed here: SU2 Solver. Mesh Description:

The mesh for the flat plate that has been used in the SU2 code is made up of quadrilateral nodes, 65 in number in both x and y directions. They are not uniform but are concentrated along the wall (y = 0) and starting at x = 0 m and are of length 0.3048 m (1 ft).

In figure 1, the Navier-Stokes no-slip boundary condition is marked in green. The domain extends a distance upstream of the flat plate, and a symmetry boundary condition is used to simulate a free-stream approaching the plate in this region (highlighted in purple). Axial stretching of the mesh is used to aid in resolving the region near the start of the plate where the no-slip boundary condition begins at x = 0 m.

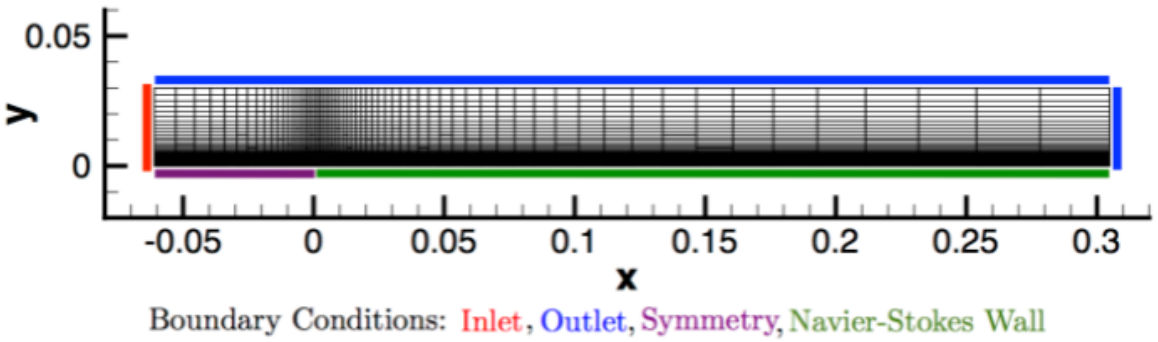

Fig. 1: Mesh and boundary conditions for SU2

3. RESULTS & DISCUSSION

3.1 BASE FLOW

Table 1: Flow parameters (input to SU2)

L (length) (m)	Free stream U (m/s)	Viscosity (kg/m-s)	Density (kg/m3)	Free stream Re	Abbreviation
0.3048	70	1.83E-03	1.2886	1.50E+04	f3
0.3048	70	1.83E-04	1.2886	1.50E+05	f4
0.3048	70	1.83E-05	1.2886	1.50E+06	f5
0.3048	70	9.06E-04	1.2886	3.03E+04	f11

The SU2 code came with a fixed free stream velocity value of 70m/s, therefore, to get the profiles at different Reynolds numbers, the viscosity of the flow was changed and the code was run. Table 1 tabulates the different Reynolds numbers for which the flow profile was obtained. The output from the SU2 code was imported into **Paraview Software** for the visualisation part. In the Paraview software, appropriate tools were used to get the entire flow profile of the flat plate for the entire domain, and exported the data into csv files to plot the **flow profile** on MATLAB.

Two sets of plots were plotted, one for velocity at different streamwise locations for the different Reynolds numbers and the other, comparison of the velocity at the exit plane x = 0.3048 m for various Reynolds numbers. The graphs are as follows.

3.1.1 SU2

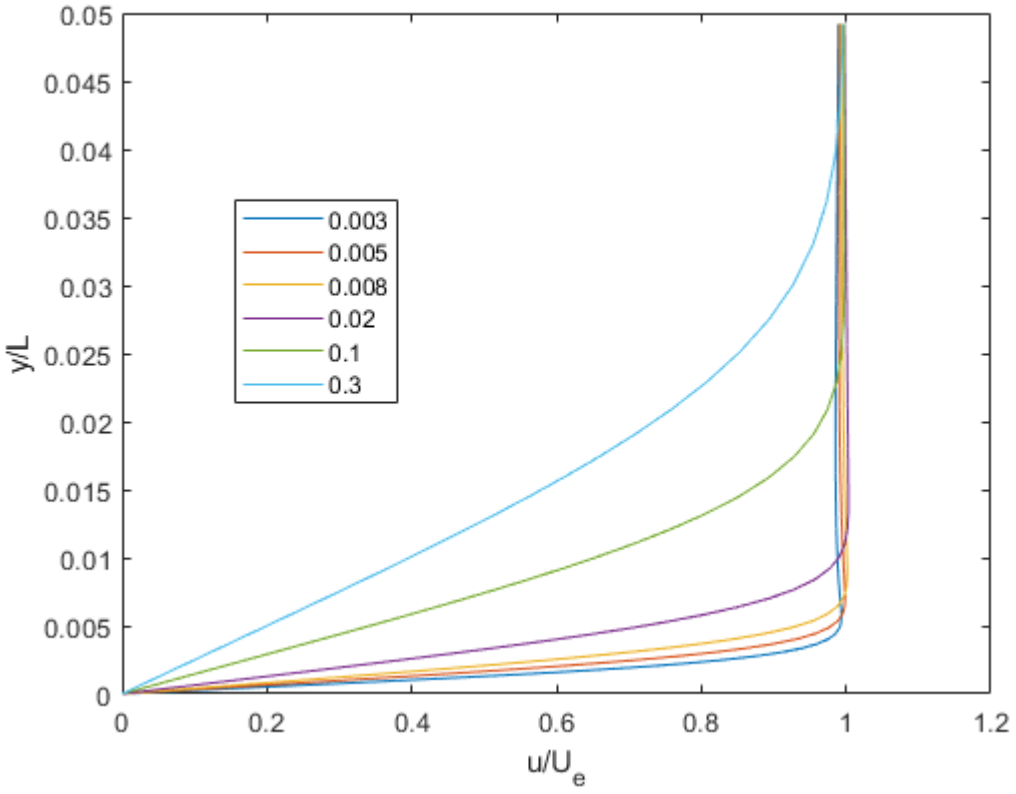
0.05
0.045
0.04
0.035
0.03
0.025
0.02
0.015
0.01
0.005
0
y/L
0.003
0.005
0.008
0.02
0.1
0.3
0
0.2
0.4
0.6
0.8
1
1.2
u/U_e

a)

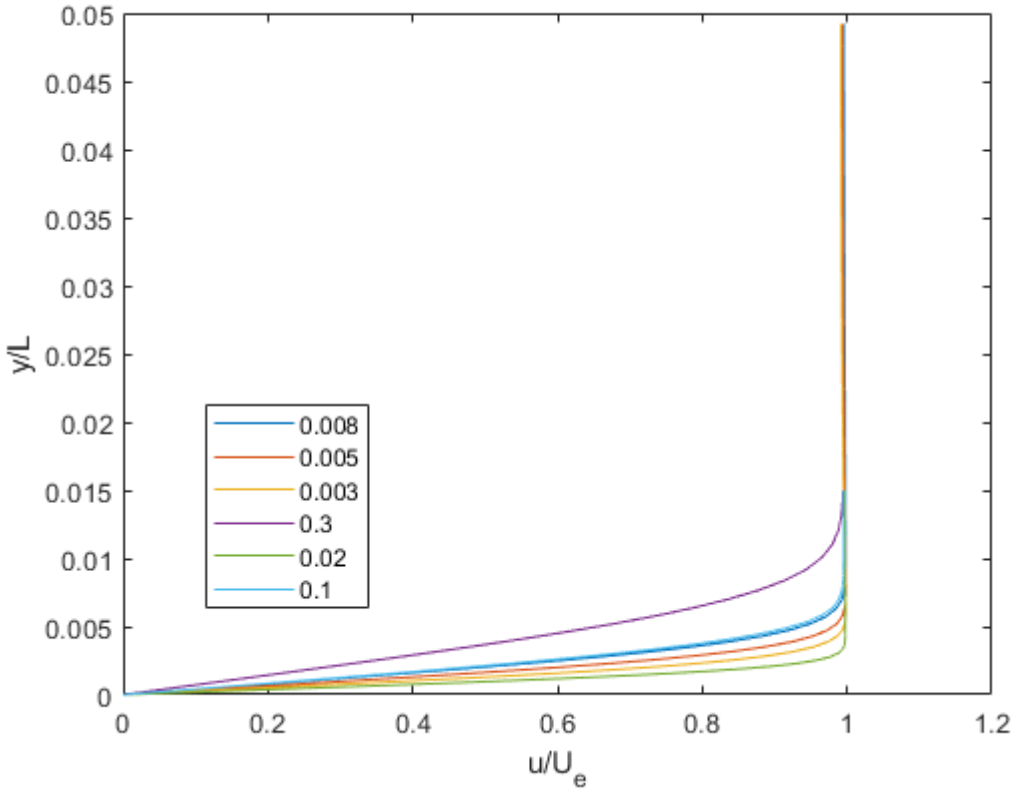
0.05
0.045
0.04
0.035
0.03
0.025
0.02
0.015
0.01
0.005
0
y/L
0.008
0.005
0.003
0.3
0.02
0.1
0
0.2
0.4
0.6
0.8
1
1.2
u/U_e

b)

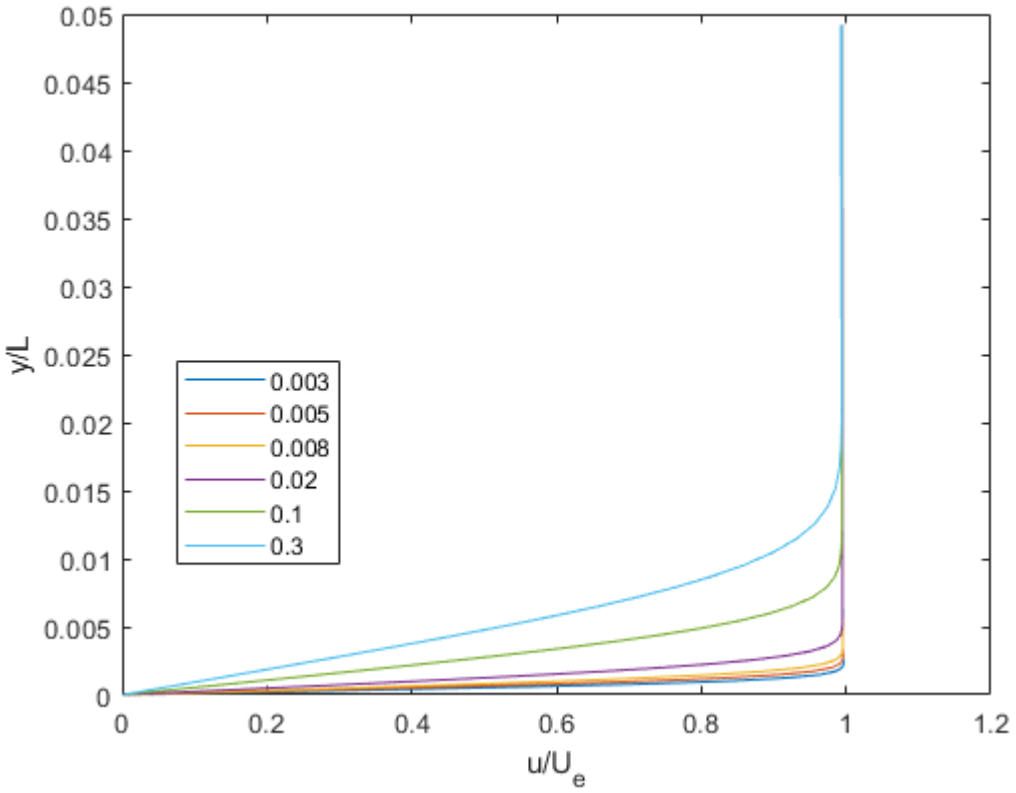

c)

Fig 2: Velocity at different streamwise locations for a) f3 b) f4 c) f5

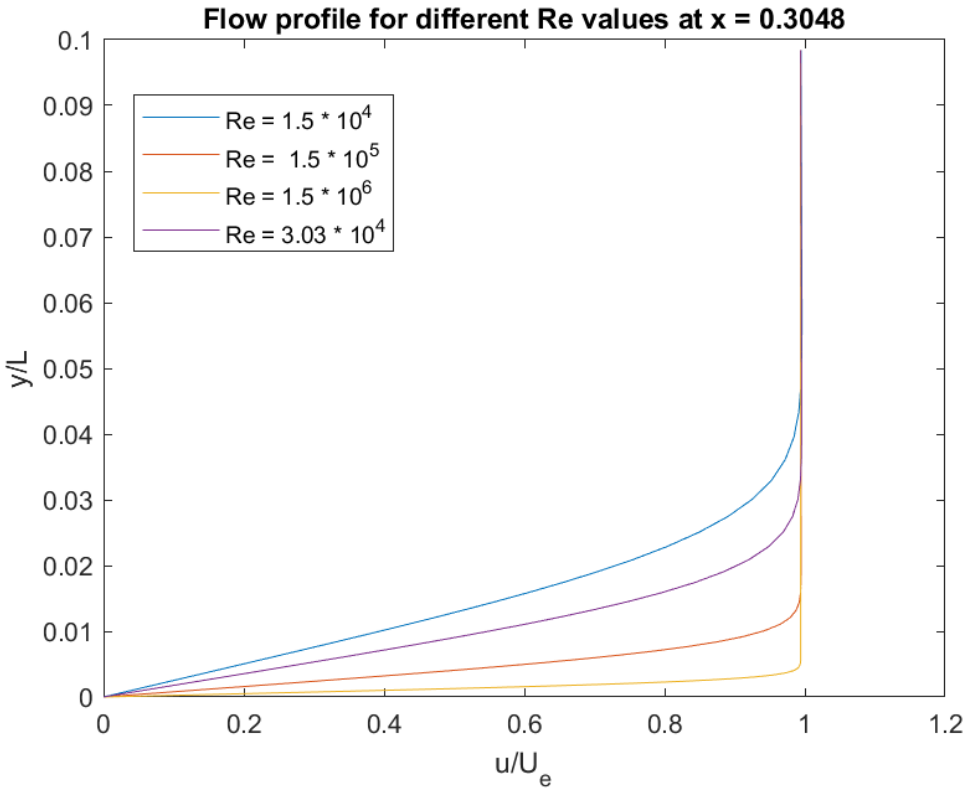

Fig 3: Velocity at the exit plane x = 0.3048 m for various Reynolds numbers

3.1.2 Blasius Profile

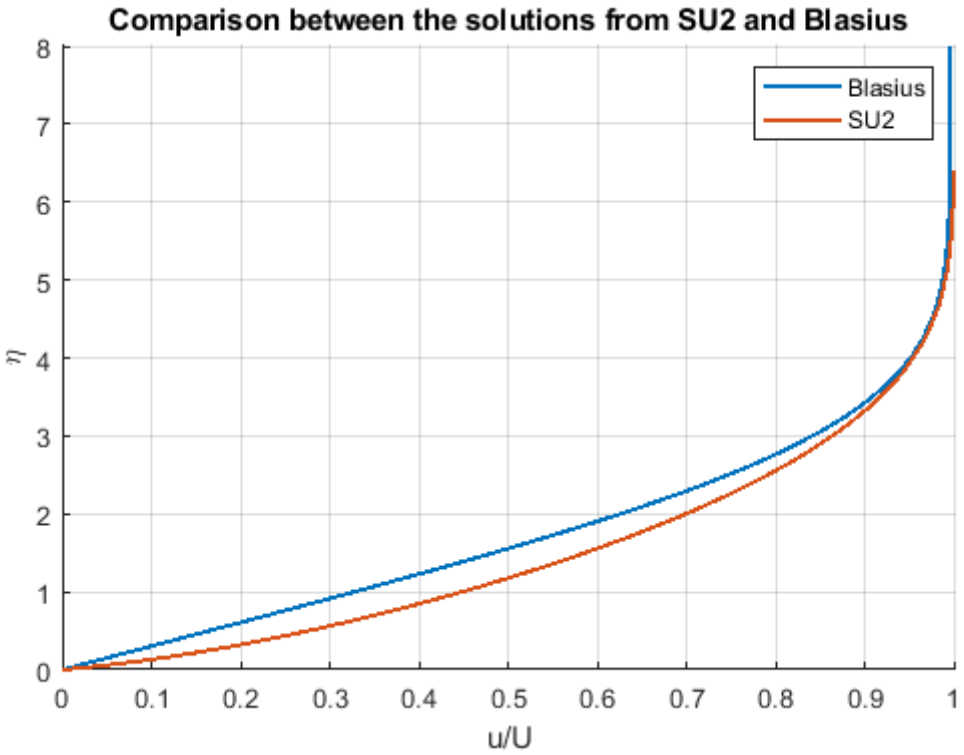

Fig. 4: Comparison of similarity variable eta for Blasius profile and SU2 solution at the exit plane of the mesh (x=0.3048 m) near the wall for f5

The SU2 profile and Blasius profile are shown in figure 4. The SU2 profile is slightly different from the Blasius profile in terms of the shape factor, however, it retains the physical properties of a typical laminar boundary layer. This deviation from the theoretical values may be attributed to the fact that the flow is simulated over a finite domain.

3.2 STABILITY ANALYSIS

3.2.1 Local Temporal Stability Analysis

Governing equations for parallel flow:

$$\frac{\partial u}{\partial x} + \frac{\partial v}{\partial y} + \frac{\partial w}{\partial y} = 0 \tag{1}$$

$$\frac{\partial u}{\partial t} + U(y)\frac{\partial u}{\partial x} + v\frac{\partial U}{\partial y} = -\frac{\partial p}{\partial x} + \frac{1}{Re}\nabla^2 u \tag{2}$$

$$\frac{\partial v}{\partial t} + U(y)\frac{\partial v}{\partial x} = -\frac{\partial p}{\partial y} + \frac{1}{Re}\nabla^2 v \tag{3}$$

$$\frac{\partial w}{\partial t} + U(y)\frac{\partial w}{\partial x} = -\frac{\partial p}{\partial z} + \frac{1}{Re}\nabla^2 w \tag{4}$$

Perturbations:

$$\underrightarrow{u}(x,y,z,t) = \underrightarrow{\hat{u}}(y)e^{ik_x x + ik_z z}e^{-i\omega t} \tag{5}$$

The Navier-Stokes equations can be simplified by taking a parallel flow assumption. We introduce perturbations of the form as given in equation (5). On linearizing this set of equations about the base flow (say U = U(y)) we get four equations in perturbation quantities, velocity (u,v,w), vorticity and pressure. These equations can then be reduced into two evolution equations in v (the vertical component of velocity) and vorticity by eliminating u,v and p. This form is also referred to as the velocity-vorticity formulation. (Equation 6 and 7)

Orr-sommerfeld equation

$$(U(y)-c)\left(\frac{\partial^2 \hat{v}}{\partial y^2} - (k_x^2 + k_z^2)\hat{v}\right) - \frac{d^2U}{dy^2}\hat{v} = \frac{1}{ik_x Re}\left(\frac{d^2}{dy^2} - (k_x^2 + k_z^2)\right)^2 \hat{v} \tag{6}$$

Squire's equation

$$(U(y)-c)\hat{\omega}_y - \frac{1}{ik_x Re}\left(\frac{d^2}{dy^2} - (k_x^2 + k_z^2)\right)\hat{\omega}_y = -\frac{k_z}{k_x}\frac{dU}{dy}\hat{v} \tag{7}$$

This set of equations can be represented in the matrix form.

$$L\,\underrightarrow{q} = i\omega M\,\underrightarrow{q}$$

i.e.

$$-i\omega \begin{bmatrix} k^2 - D^2 & 0 \\ 0 & 1 \end{bmatrix} \begin{bmatrix} \hat{v} \\ \hat{\omega}_y \end{bmatrix} + \begin{bmatrix} L_{OS} & 0 \\ i\beta U' & L_{SQ} \end{bmatrix} \begin{bmatrix} \hat{v} \\ \hat{\omega}_y \end{bmatrix} = 0 \tag{8}$$

where, U = U(y) = base flow profile, $k^2 = k_x^2 + k_z^2$,

$$L_{OS} = i\alpha U(k^2 - D^2) + i\alpha U'' + \frac{1}{Re}(k^2 - D^2)^2 \qquad L_{SQ} = i\alpha + \frac{1}{Re}(k^2 - D^2)$$

Equation (8) is of the form of an eigenvalue problem AX = λBX, and the eigenvalues for our formulation are of the form: λ = iω. This eigenvalue problem was solved for the flow velocity profiles obtained in Section 3.1.1. Here, the domain is discretized using the Gauss-Lobatto-Chebyshev points, such that more nodes are present near the wall to capture the boundary layer. Eigenvalue and eigenfunction plots are presented as follows.

NOTE: Eigenmodes (λ = iω) are stable if the real part of the eigenvalue is positive which is evident by the exponent e-λt multiplied to the perturbation (equation 5).

Eigenmodes

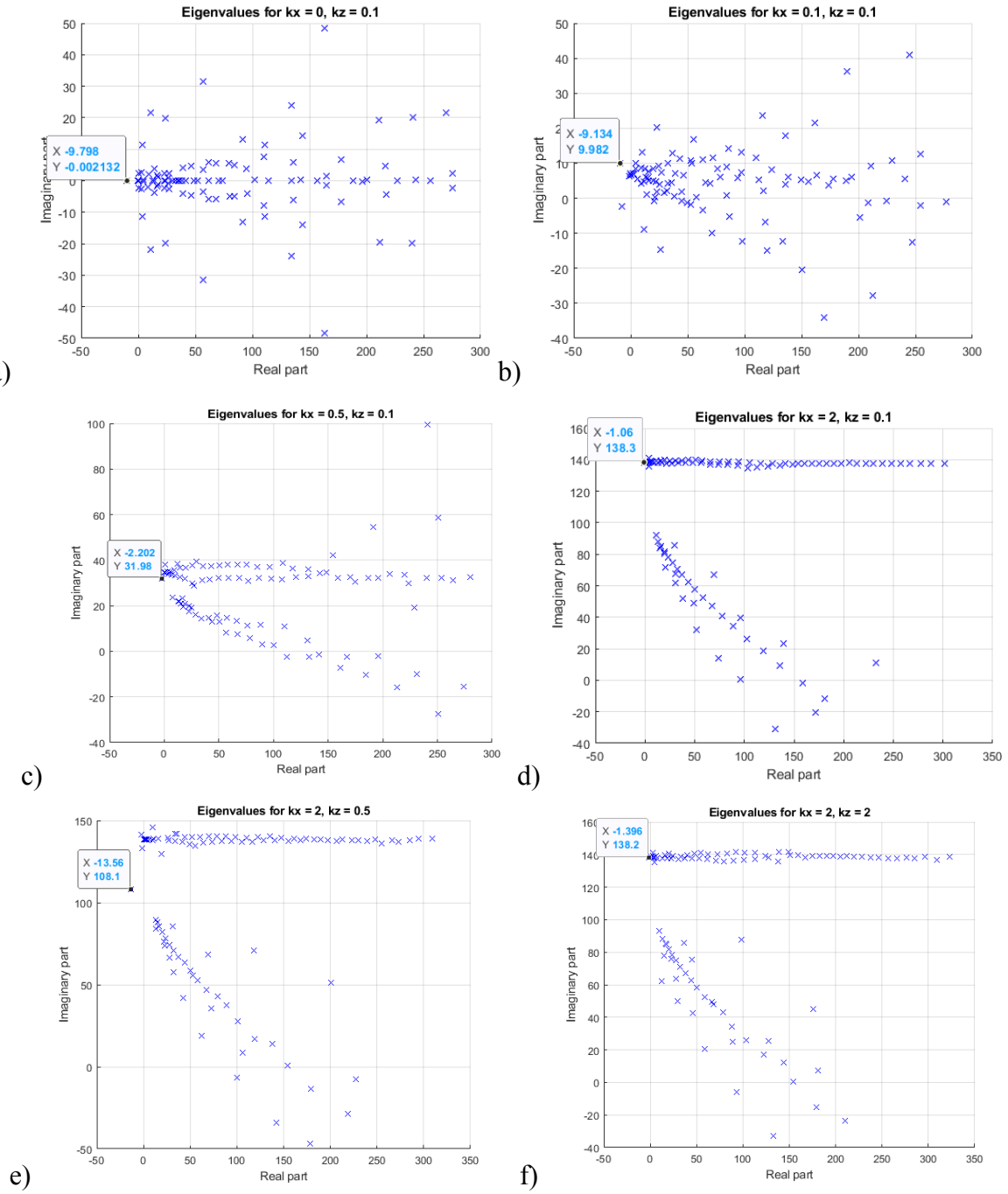

Fig. 5: Eigenvalues for flow Re = 1.5 x 10^5 at x = 0.1 from leading edge

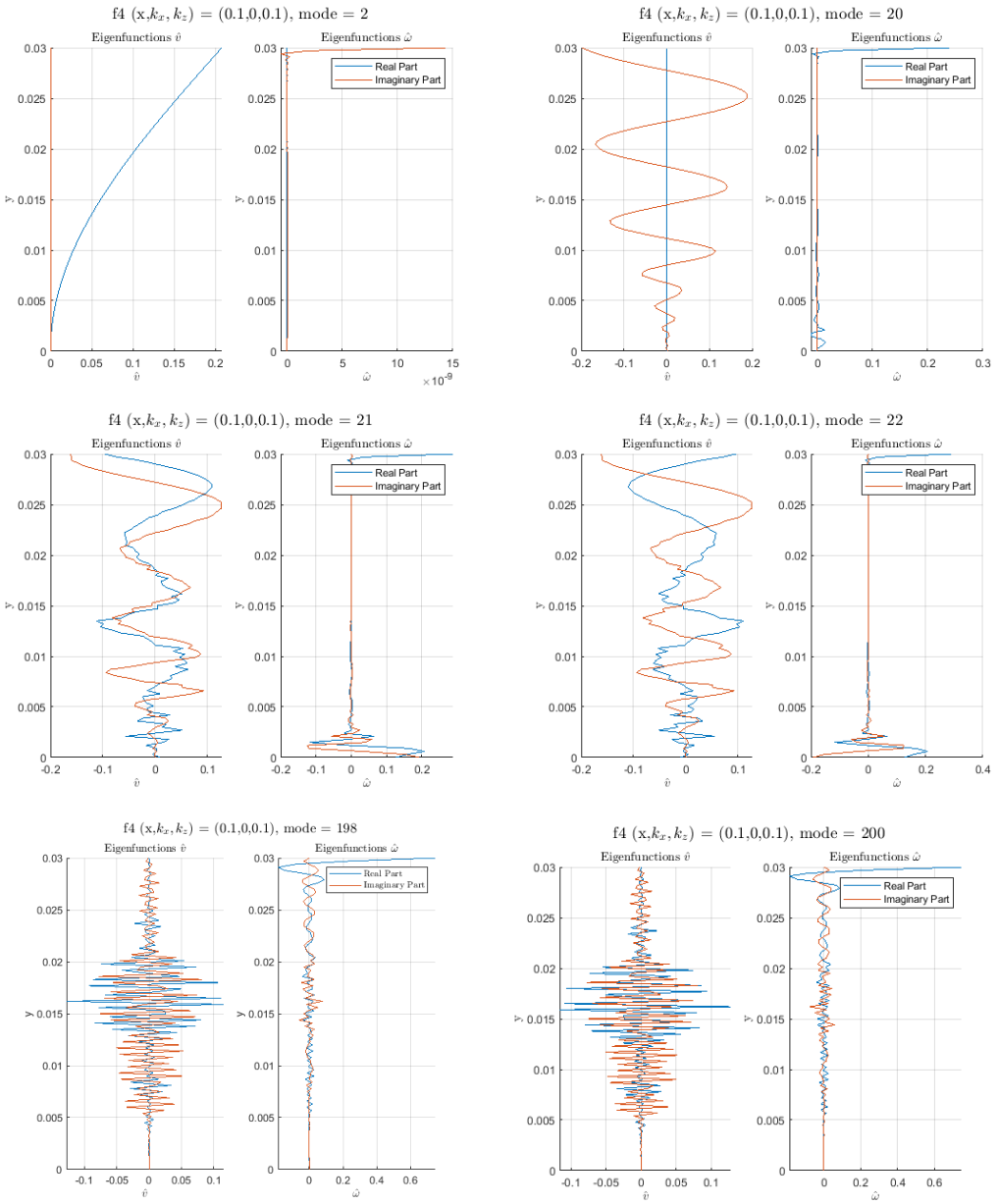

Fig. 6: Eigenfunctions for x = 0.1m, k_x = 0, k_z = 0.1, Re = 1.5 x 10^5 (f4) (figure 5a)

Table. 2: Eigenmodes used in figure 6

Mode	lambda r	lambda i
2 (OS)	2.96E+11	0.00E+00
20 (OS)	1.71E+04	-1.23E-05
21 (OS)	1.44E+04	-6.03E+03
22 (OS)	1.44E+04	6.03E+03
198 (SQ)	2.95E+01	-1.49E+00
200 (SQ)	2.94E+01	1.49E+00

OS = Orr-Sommerfeld, SQ = Squire's

Figure 5 shows the Squire eigenspectra for the flow at Re = 1.5×10^5 at the streamwise location of x = 0.1m from the leading edge. On varying the spanwise and the streamwise wave numbers we can infer:

1. The eigenspectrum is almost symmetric about the imaginary axis when $k_x = 0$. To verify this, the eigenvectors are plotted in figure 6.
2. As the streamwise wavenumber increases, the eigenvalues separate out into two branches.
3. The branch with an almost constant imaginary part can be interpreted as the continuous spectrum. These results can be compared with those reported in the literature (figure 9)
4. The eigen spectrum was again plotted for the same wavenumber, but at different streamwise locations. This is shown in figure 7.
5. For the same k_x and k_z, the most unstable eigenmode decreases as we move away from the leading edge in a streamwise direction.
6. For a better understanding of the variation of the most unstable mode corresponding to a fixed k_x and varying k_z, see figure 8.
7. The real part of the most unstable eigenmode becomes less negative as the k_x increases (for $k_z = 0.1$). This means that as the streamwise wavenumber increases, the flow becomes less unstable.

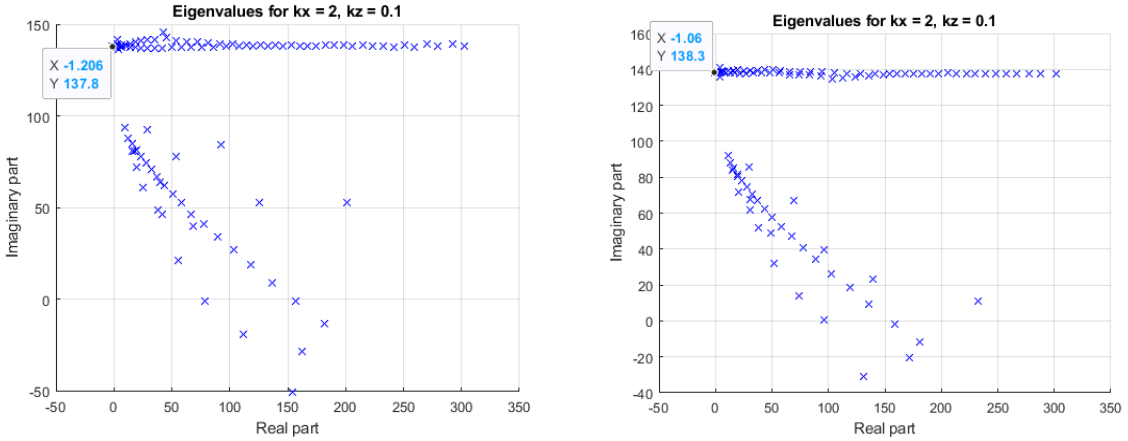

Fig. 7: x = 0.003 (left) and x = 0.1 (right) for f4

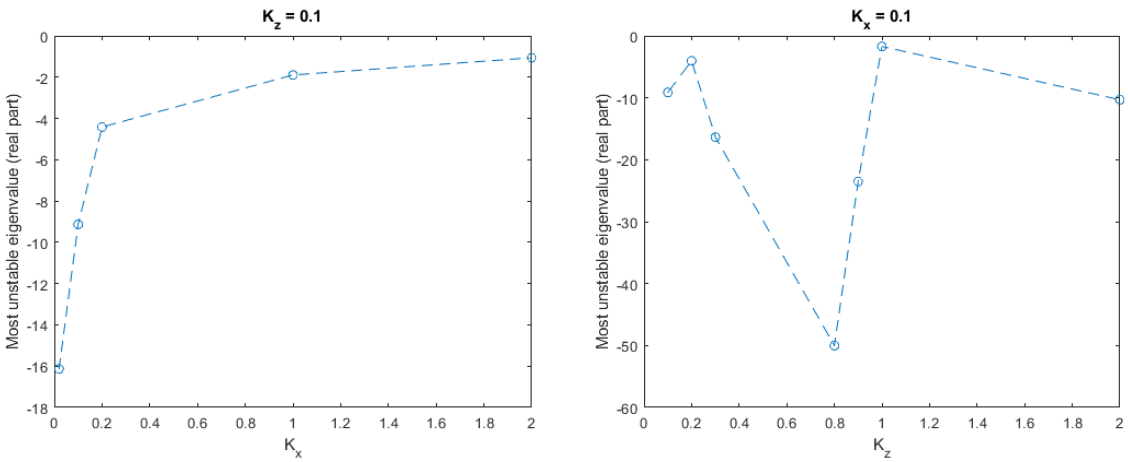

Fig. 8: Variation of the real part of the most unstable squire mode

$$(D^2 - \alpha^2)^2 \phi = i\alpha R \left[(u - c)(D^2 - \alpha^2)\phi - \phi D^2 u \right]$$

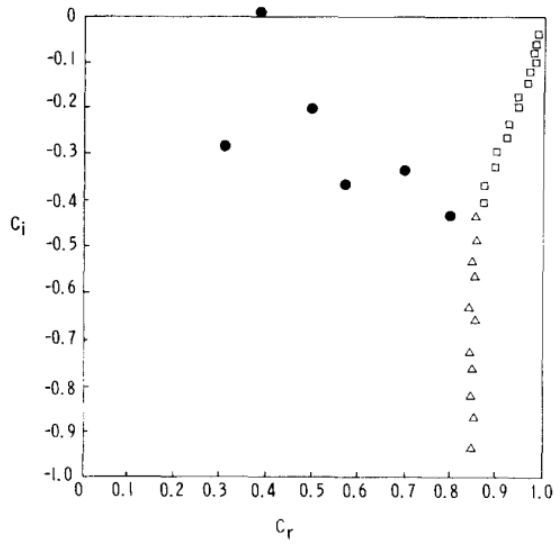

Fig. 9: Distribution of eigenvalues for the Blasius boundary layer flow at α=0.308, Re = 998 (different symbols represent different families) ((Antar & Benek, 1978))

3.2.2 Spatial: CMM using Cubic Profile

For the spatial stability analysis, we need to consider the following Orr-Sommerfeld equation (wavenumber, α, frequency, ω_o and non-dimensionalized stream function ϕ):

$$\phi^{iv} - 2\alpha^2\phi^{ii} + \alpha^4\phi = iRe[(\alpha - \omega_o)(\phi^{ii} - \alpha^2\phi)] \tag{9}$$

with the boundary conditions given by:
At y = 0: f, $\phi = 0$
As y→∞: f, $\phi \rightarrow 0$
As y→∞: U(y) = 1
As y→∞: U''(y) = 0
Also,
$\phi' = -i\alpha f$
U is taken as cubic velocity profile

Solving which we get:

$$\phi = a_1\phi_1 + a_2\phi_2 + a_3\phi_3 + a_4\phi_4 \tag{10}$$

where

ϕ_1 is $e^{-\alpha y}$; ϕ_2 is $e^{\alpha y}$; ϕ_3 is e^{-Qy} ; ϕ_4 is e^{Qy}

$$Q = [\alpha^2 + i\alpha Re(1 - c)]^{1/2}$$

ϕ_2 and ϕ_3 are dropped out, as y→∞: f, $\phi \rightarrow 0$.
So, we are left with

$$a_1\phi_1(y = 0) + a_3\phi_3(y = 0) = 0$$
$$a_1\phi_1'(y = 0) + a_3\phi_3'(y = 0) = 0$$

which gives the dispersion relation

$$(\phi_1\phi_3' - \phi_3\phi_1')_{y=0} = 0 \tag{11}$$

Since, this is a stiff differential equation, we define a new set of variables:

$$Y = [y_1 \; y_2 \; y_3 \; y_4 \; y_5 \; y_6]^T$$

where,

$$y_1 = \phi_1\phi_3' - \phi_3\phi_1'$$
$$y_2 = \phi_1\phi_3'' - \phi_3\phi_1''$$
$$y_3 = \phi_1\phi_3''' - \phi_3\phi_1'''$$
$$y_4 = \phi_1'\phi_3'' - \phi_3'\phi_1''$$
$$y_5 = \phi_1'\phi_3''' - \phi_3'\phi_1'''$$
$$y_6 = \phi_1''\phi_3''' - \phi_3''\phi_1'''$$

And the new set of ODE can be re-written as:

$$\frac{\partial Y}{\partial y} = AY \tag{12}$$

where

$$A = \begin{bmatrix} 0 & 1 & 0 & 0 & 0 & 0 \\ 0 & 0 & 1 & 1 & 0 & 0 \\ 0 & b_1 & 0 & 0 & 1 & 0 \\ 0 & 0 & 0 & 0 & 1 & 0 \\ b_2 & 0 & 0 & b_1 & 0 & 1 \\ 0 & b_2 & 0 & 0 & 0 & 0 \end{bmatrix}$$

$b_1 = 2\alpha + iRe\alpha(U - c)$

$b_2 = \alpha^4 + i\alpha^3 Re(U - c) + i\alpha ReU''$

with initial condition

$$Y_\infty = [1 \quad -(\alpha + Q) \quad (\alpha^2 + \alpha Q + Q^2) \quad \alpha Q \quad -\alpha Q(\alpha + Q) \quad \alpha^2 Q^2]$$

This system has been solved step wise in MATLAB with ∞ conditions applied at 10δ (10 times boundary layer thickness) for step-sizes 0.1δ and 0.01δ, then we put

$$\Re(y_1) = 0, \text{Imag}(y_1) = 0$$

to get α_R and α_I. Here $\Re(*)$ and Imag(*) denotes real and imaginary parts of * respectively.

Result Analysis and Grid convergence

The above equations were solved for 6 different Re_{δ^*}

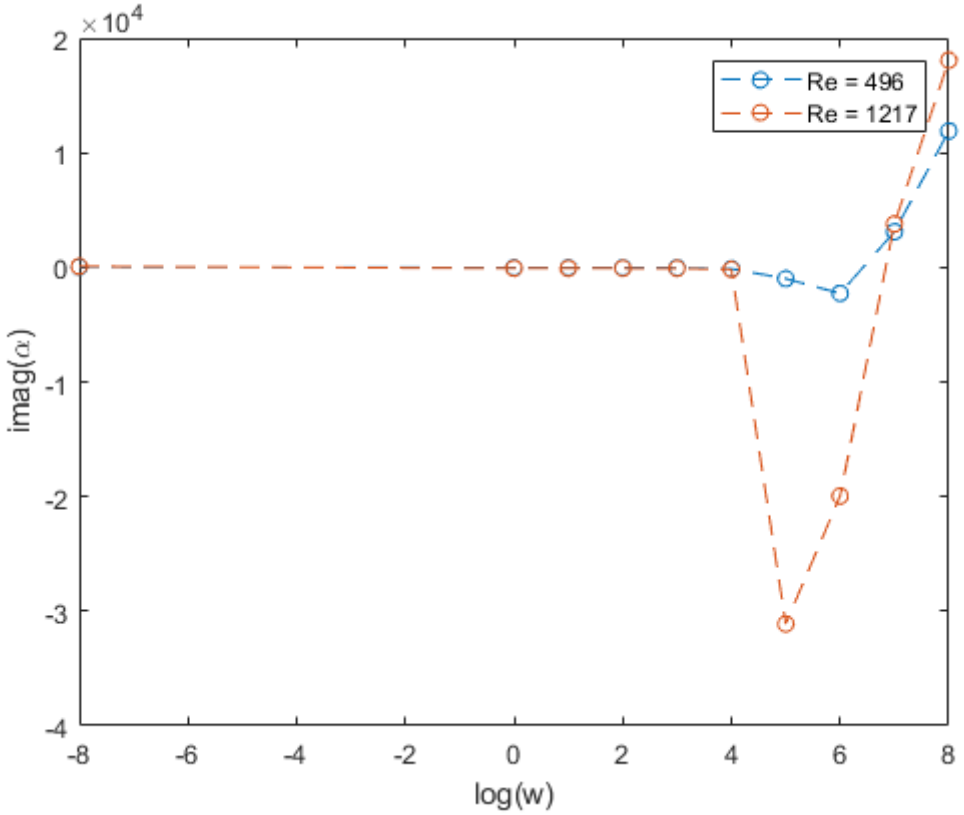

Fig. 10: α-ω plot for Re = 496 and Re = 1217 with h = 0.01δ

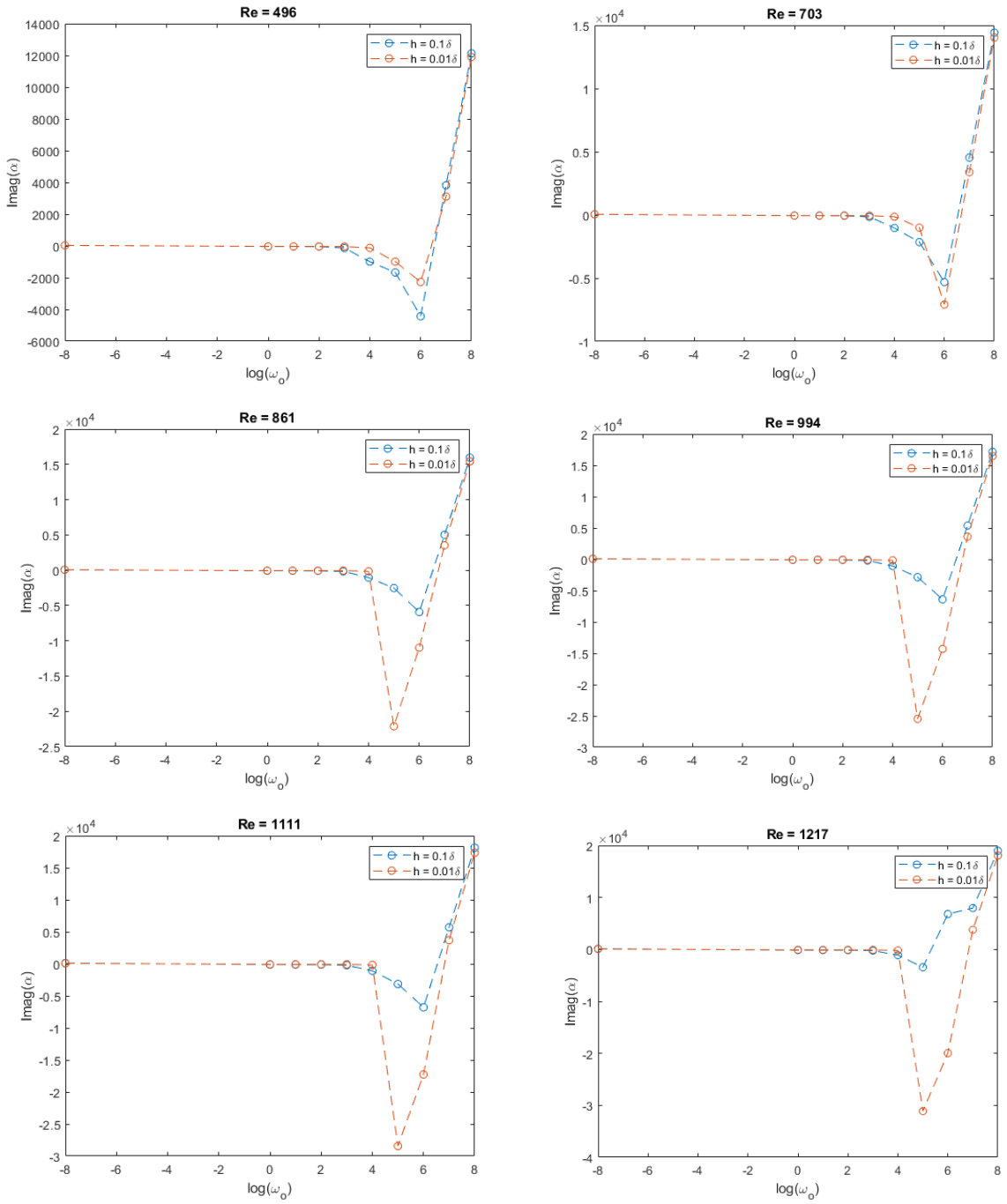

Fig. 11: α-ω plots for $Re_{\delta*}$ = a) 496 b) 703 c) 861 d) 994 e) 1111 f) 1217 with h = 0.01δ and h = 0.1δ

From the above figures, we can infer the following:

1. Step-size = 0.1δ gives very low error for low Reynolds number but is not appropriate as the error is huge for higher Reynolds number.
2. The most unstable eigenvalue lies in between the unstable range (negative α_I) and not at the boundaries.
3. Most unstable eigenvalue increases with Reynolds number initially increases at high rate and then saturates.
4. The unstable regime almost remains constant in terms of the angular frequency.

5. Errors are large for these two step-sizes whenever there is a jump in the value(abrupt deviation from a straight line behaviour).
6. The unstable regime is small and the unstable eigenvalues are also small for Re_{δ^*} = 496 as compared to that for Re_{δ^*} = 1217 and it implies that Re = 496 is close to the critical Reynolds number and the thumb structure of the plot limits its unstable eigenvalues as well as its range.

3.3 RECEPTIVITY

3.3.1 Concept

One peculiar observation about the stability/eigenvalue analysis is it requires neither the knowledge of excitation fields nor the wall normal location, where it is applied. In eigenvalue analyses, excitation field information is obscured through the application of homogeneous conditions at the boundaries. One needs to keep this information while doing a hydrodynamic analysis.

In addition to this, one needs to take care of the free stream excitations as well. In the stability analyses, we talked only about the wall mode disturbances. Free stream excitation gives rise to another important question: the coupling mechanism between free stream and wall mode excitation.

All of this gives rise to a new technique to analyse the problem, receptivity. The idea is to see the problem in the form :

$$Y(\omega_o) = T(\omega_o)X(\omega_o)$$

where

Y is the output to an input given to a dynamical system modeled by the transfer function T. This allows us to get a deep insight into the hydrodynamic analysis and eradicate the above mentioned defects as well.

3.3.2 Theoretical Approach

As mentioned in section 1, we first explore the concept of receptivity with a model problem. The following equation is an ODE representing simple harmonic motion with forcing term.

$$\frac{\partial^2 u}{\partial x^2} + \omega^2(x)u = cos\Omega x \tag{13}$$

For simplicity, the frequency is taken as ω(x) = x/2 + pi for demonstration. The behavior of such a linear system is dominated initially by the particular solution, and the system oscillates with the frequency Ω.

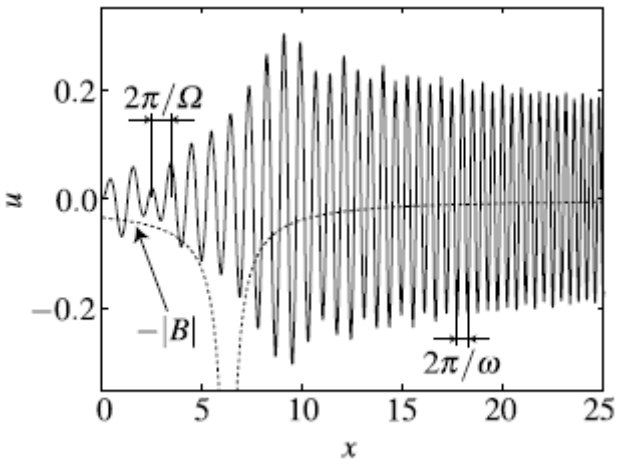

Fig. 12: Forced Harmonic oscillator (Schmid & Henningson 2001)

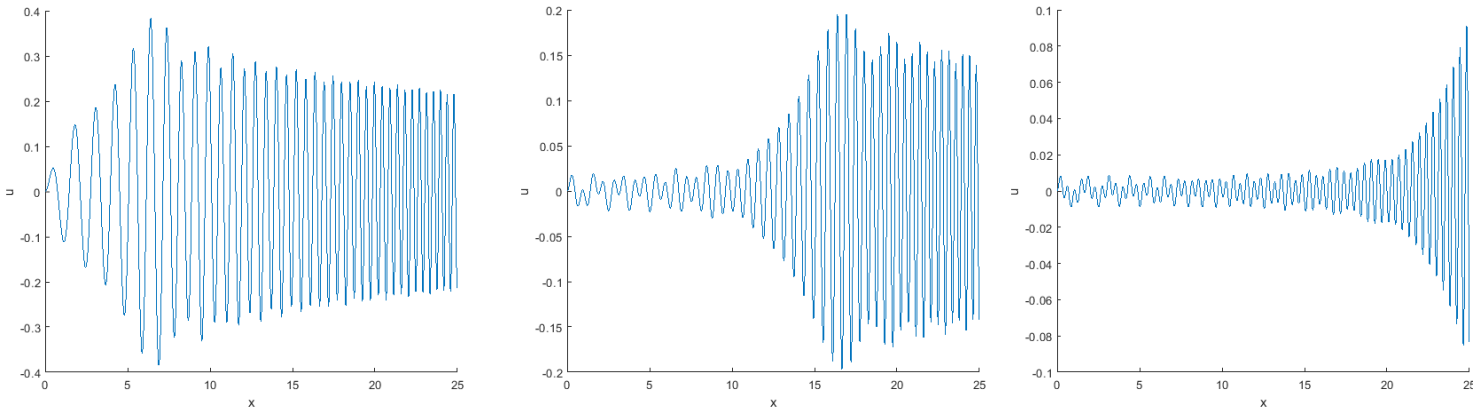

Fig. 13: Forced Harmonic oscillator plots for Ω = 5,10,15

Figure (13) shows the response of the ODE as the frequency is changed, for different values of Ω. The maximum amplitude is observed near the value of x such that $\omega(x_0) = \Omega$ at a certain x_0. This signifies resonance i.e. enhanced response of the system to a particular forcing.

This idea motivates the next section based on response of the boundary layer to certain excitations.

3.3.2 Receptivity of Boundary Layers to Wall Excitation

The basic flow problem here remains the same, we consider perturbations of small amplitude imparted to the parallel flow. However, all the formulations are now done in the Fourier space for convenience, The boundary layer is excited locally, and we analyse the response to time harmonically localized disturbance, i.e. impulse response.
In the α-ω space, the perturbation stream function can be written as

$$\psi(x,y,t) = \int_{Br} \frac{\phi_1(y,\alpha)\phi'_{30} - \phi'_{10}\phi_3(y,\alpha)}{\phi_{10}\phi'_{30} - \phi'_{10}\phi_{30}}\, e^{i(\alpha x - \bar{\omega}_0 t)}\, d\alpha \tag{14}$$

(variables are as defined in section 3.2.2.)

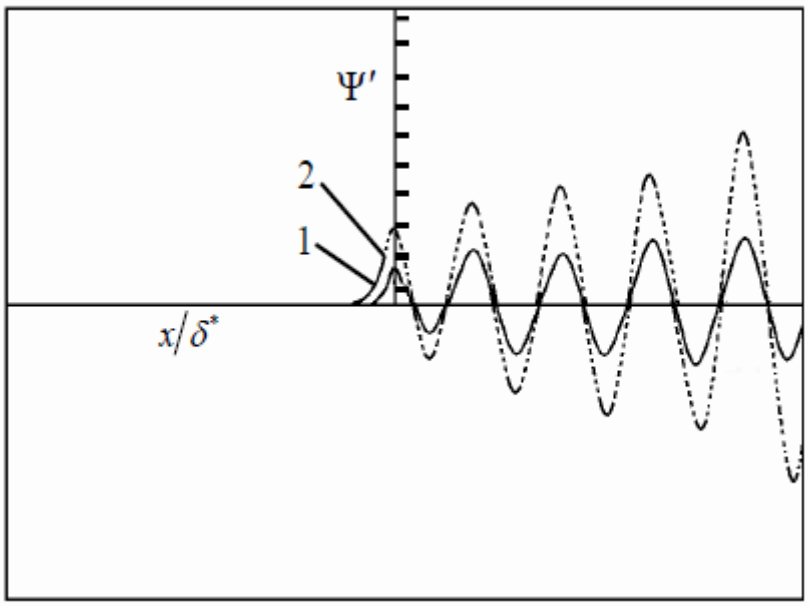

Fig. 14: Disturbance stream function plotted versus streamwise distance for (1) the inner maximum at $y/\delta^* = 0.277$ and (2) the outer maximum at $y/\delta^* = 1.79$. (Sengupta 2012)

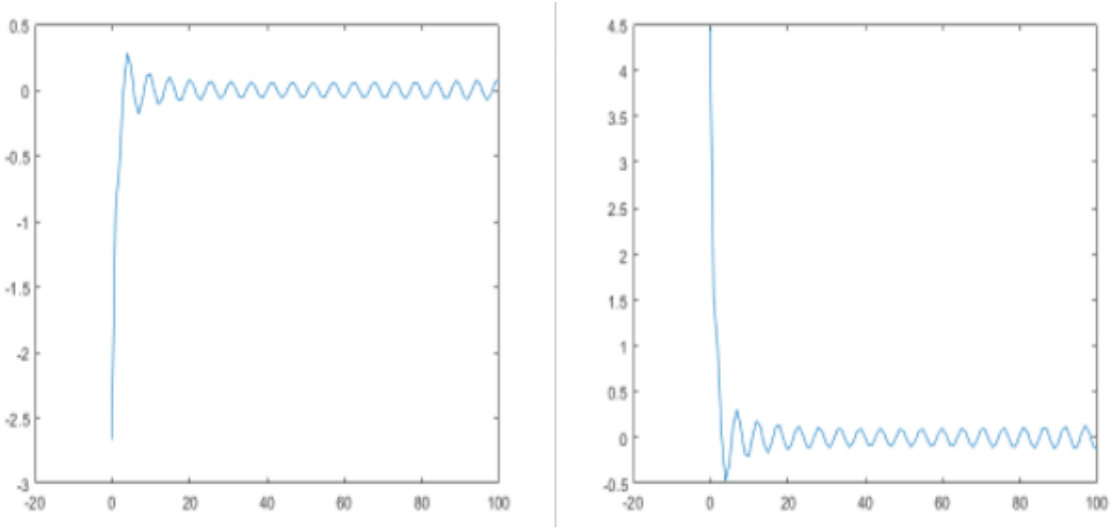

Fig. 15: Plot of disturbance stream function (Ψ) vs x for Re = 1000 (left) and Re = 400 (right) at the outer maxima

For the above plots, the vibrating ribbon is assumed to be placed at x =0 and as expected, receptivity analysis provides a solution which has a sharp jump at x = 0. However, this jump is of the opposite sign in both cases. The sign or direction of the jump depends on the time at which we are calculating the function. This is one of the issues not addressed in the stability analysis. When we calculate, peak to peak value of the oscillations, the oscillations tend to die out for $Re_{\delta^*} = 400$ whereas they tend to grow for $Re_{\delta^*} = 1000$. These features can be seen in the plot below as well.

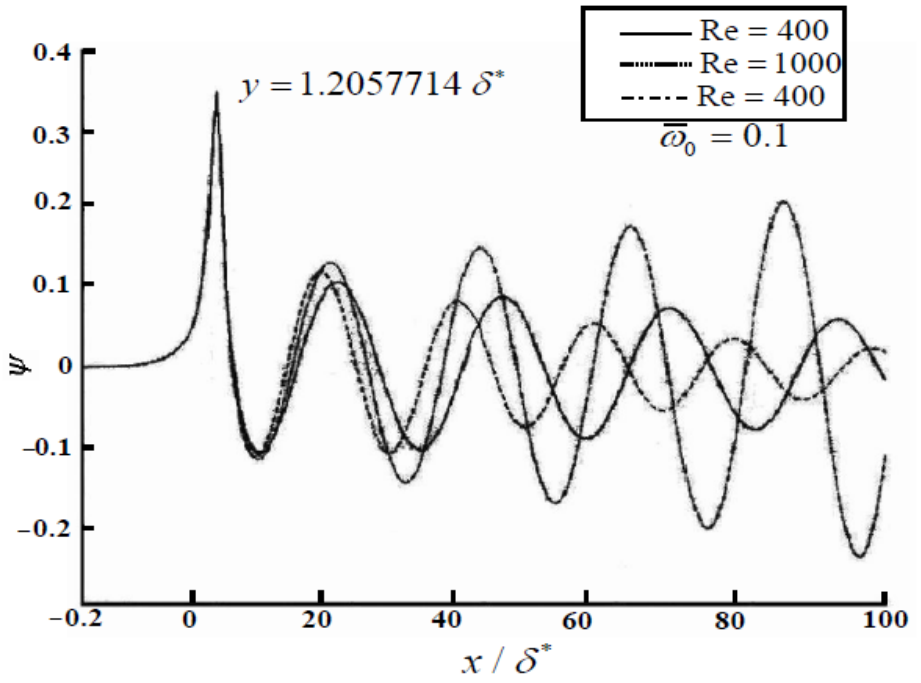

Fig. 16: Solution of the signal problem for $Re_{\delta^*} = 1000$ and $\omega_o = 0.1$ (Sengupta 2012)

Near field response by localized excitation

The near field response can be qualitatively studied. Inspecting the nature of the solutions of asymptotic form of the Orr-Sommerfeld at $|\alpha| \to \infty$ gives more information regarding what is happening near the excitor. Introduce a small parameter $\epsilon_1 = 1/\rho$ such that $\varrho = |\alpha|$ and

$$e^{i\theta} = \rho\beta \tag{15}$$

$$\begin{aligned}&\epsilon_1^4\,\phi^{iv} - [2\epsilon_1^2\,\beta^2 + iRe\,\epsilon_1^3\,(\beta U - \epsilon_1\,\bar{\omega}_0)]\,\phi'' \\ &+ [\beta^4 + iRe\,\beta\epsilon_1^3\,U'' + iRe\,\beta^2\epsilon_1\,(\beta U - \epsilon_1\,\bar{\omega}_0)]\,\phi = 0\end{aligned} \tag{16}$$

and boundary conditions:

$$y = 0: \qquad u = 0 \quad \text{and} \quad \psi(x,0,t) = \delta(x)\,e^{-i\bar{\omega}_0 t} \tag{17}$$

Note: Equation 16 is a *Singular Perturbation Problem*. The outer solution is $\phi_0 = 0$ and inner solution:

$$\begin{aligned}&\left(\frac{\epsilon_1}{\delta}\right)^4 \phi_i^{iv} - \left[2\beta^2\left(\frac{\epsilon_1}{\delta}\right)^2 + iRe(\beta U - \epsilon_1\bar{\omega}_0)\left(\frac{\epsilon_1^3}{\delta^2}\right)\right]\phi_i'' \\ &+ \left[\beta^4 + iRe\beta\epsilon_1^3 U'' + iRe\beta^2\epsilon_1(\beta U - \epsilon_1\bar{\omega}_0)\right]\phi_i = 0\end{aligned} \tag{18}$$

which on integrating along the Bromwich contour gives

$$\begin{aligned}\psi(x,y,\rho,t) = &\left[e^{-\rho x}\cos\rho y + \frac{ie^{i\rho z}}{z}\left(1 + \rho y + \frac{iy}{z}\right) - \frac{ie^{-i\rho\bar{z}}}{\bar{z}}\left(1 + \rho y - \frac{iy}{\bar{z}}\right)\right. \\ &\left. - \frac{ie^{\rho z + iz}}{z}\left(1 + \frac{iy}{z} + i\rho y + y\right) + \frac{ie^{-\rho\bar{z} - i\bar{z}}}{\bar{z}}\left(1 - \frac{iy}{\bar{z}} - i\rho y + y\right)\right]\frac{e^{-i\bar{\omega}_0 t}}{2\pi}\end{aligned} \tag{19}$$

In the limit, $|\alpha| \to \infty$, the first and third terms in the above do not contribute. The second term in the equation (19) turns out to be the Dirichlet function, which is an approximation of the delta function.

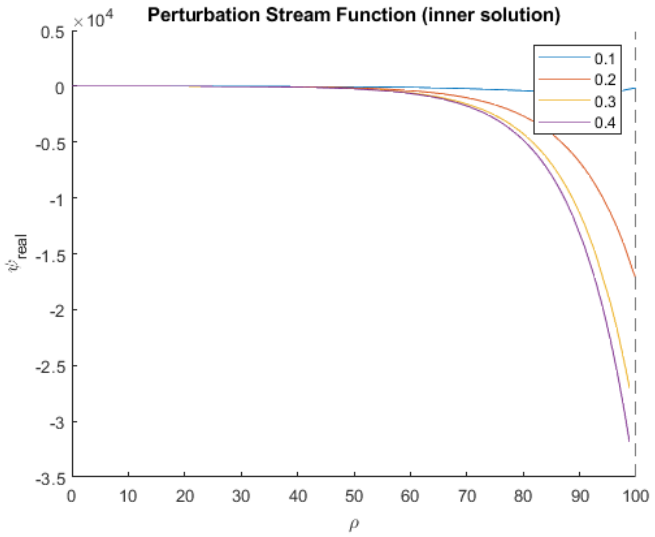

Fig. 17: Plot of $\Re(\Psi)$ vs ϱ

$\Re(*)$ denotes the real part of *.

As we know that the infinity in the wavenumber space corresponds to the region localized near the excitation, figure 13 clearly shows that we recover the applied boundary condition at y = 0 (i.e. ϱ large). Therefore, the delta function is totally supported by the point at infinity in the wavenumber space (which is nothing but the circular arc). The analysis gives a good picture of how the solutions of Bromwich contour are valid. Moreover, this brings forward the fact that for a physically realistic problem, the localized excitor would be a finite source. So, the mathematical implementation of $|\alpha| \to \infty$ may not be possible. Instead, there would exist a finite α (i.e. cut-off wavenumber).

4. CONCLUSION

- The report brings forth an attempt to explore application-based study of the boundary layer theory, considering a simpler case - boundary layer over a flat plate.
- The topics covered extend from calculating for the base flow profile, implementation of the stability theory for the same, and receptivity of the boundary layer over a flat plate.
- The results from the local stability analysis showed a good resemblance with those reported in the literature. However, the analysis can be made better by using appropriate computational resources. Grid refinement and other techniques may be implemented.
- The CMM technique is a clever wrap-around method for solving the Orr-Sommerfeld equation. With the advancement in technology we can now solve such problems with other direct techniques as well.
- CMM didn't produce the correct value of α_I , but the result follows all the trends that α_I shows theoretically.
- Given a faster processor, results for more refined mesh and larger domain could have been computed for CMM.
- Receptivity analysis shows a sharp peak at the point at which the disturbance is applied, as expected. Receptivity analysis could also have been done by applying perturbation to the Navier-Stokes equation.

5. SCOPE

- The analysis done in section 3.3.2 can be extended to a more physical problem which is a *vibrating ribbon of finite width* instead of a δ-function excitor at the wall.
- The receptivity analysis was done mainly for wall excitations. This can further be studied for external disturbances which may be present in the free-stream.
- The coupling mechanism (a salient feature of the receptivity analysis) between wall mode excitation and free stream excitation could have been studied.
- The report was restricted to the linear perturbations and excluded the study of non-linear mechanisms. On the same theoretical structure of hydrodynamic stability, transition to turbulence can also be explored.
- Spatial and temporal growth/decay of disturbances were studied separately. Spatio-temporal wave fronts can also be examined as an extension of the above theory.
- Since, airfoils are sometimes approximated as flat plates, the above theoretical developments and simulations can also be applied to airfoils. This has been implemented and is a topic of ongoing research.

6. APPENDIX

Comparing SU2 profile against Blasius Profile

```
% BLASIUS vs. SU2 PROFILE
%% Data
Vinf = 69.1;
visc = 1.83463e-3;
x = 0.3048;
rho = 1.13235; nu = visc/rho;
U = readtable('eta_f55');
U = table2array(U);

%% Blasius Solution over Flat Plate
f = zeros(4,1);
k = 0;
while k >= 0
    [eta,F] = blas(f,k);
    if round(F(end,2),2) == 1
        figure
        hold on
        plot(F(:,2),eta,'LineWidth',1.5);
        xlabel("f'");
        ylabel('eta');
        break
    else
        k = k+0.01;
    end
end

%% Similarity Parameter for Data Input
for i = 1:1000
    y = (0.03/1000)*i;
    etanew(i) = y*sqrt(Vinf*U(i)/(x*nu));
end

% NOTE: Plot for eta < 8
plot(U(1:57),etanew(1:57),'LineWidth',1.5) % for flow F5
grid on
xlim([0,1.002])
ylim([0,8.026])
title('Comparison between the solutions from SU2 and Blasius')
legend('Blasius', 'SU2')
xlabel('u/U')
ylabel('\eta')
hold off

%% FUNCTIONS
function [eta,F] = blas(~,y)
% Blasius Solution
% eta = y*sqrt(U/(x*nu))
```

```
% f' = u/U
df = @(e,f)[f(2); f(3); (-f(1).*f(3))./2];
[eta,F] = ode45(df, [0 8], [0 0 y]);
end
```

Eigenvalues using Chebyshev discretization of OSE

```
% STABILITY ANALYSIS USING CHEBYSHEV DISC.
% -- PARALLEL FLOW ASSUMPTION
% -- Eigenmodes for the v-omega formulation
% ---- 1. Orr-sommerfeld modes (first half)
% ---- 2. Squire modes (second half of the eigenvalue matrix)

%% SETUP
% Flow Parameters -- change according to
% changes done in the 'lam_flatplate_inc.cfg'
% SU2 configuration file (esp. mu0)
filename = 'C:\Users\ASUS\Desktop\AE625-turb\eigenvalues-10march\f4\0.1.csv';
xl = 0.1;
U0 = 69.1687; rho0 = 1.2886;
mu0 = 1.83463e-4; L = 0.3048;
ymax = 0.03;          % extent of the domain in y-axis (re-check)
N = 101;              % resolution of the velocity profile (change)

Re = rho0*U0*L/mu0;
deltas = 5*xl/sqrt(Re); % displacement thickness
R = (U0*rho0/mu0)*deltas; % R a/c displacement thickness
% Re = (U0*rho0*5*x/(mu0*R))^2

% Form collocated grid for the boundary layer
% Requires more points near the wall (ie y = 0)
Dy = ymax/N;
Nm = N-1;
x = ymax*(1-cos((pi/2)*(0:Nm)/Nm)');
c = [2; ones(Nm-1,1); 2].*(-1).^(0:Nm)';
X = repmat(x,1,Nm+1);

% Chebyshev differential martix
dX = X-X';                          % (re-check)
D = (c*(1./c)')./(dX+(eye(Nm+1)));  % off-diagonal entries
D = D - diag(sum(D'));              % diagonal entries
D2 = D*D;

% Extract velocity profile from paraview -- line 16
% feed the .csv obtained from 'plot over line' data
UU = readtable(filename);
U = table2array(UU((1:end),1));
U(1,1) = 0;     % enforce no-slip boundary condition
U = diag(U);    % U = U/U0;
Up = D.*U;      % dU/dy
Upp = D2.*U;    % d2U/dy2
```

```
%% MATRIX FORM and kx-kz
% Vary streamwise and spanwise wavenumbers
kx = 0; kz = 0.1; k2 = kx^2 + kz^2;

% A/c Vy-Omega Formulation
% Orr-sommerfeld matrix
KD = k2*eye(N)-D2;
Los = 1i*kx*U*KD+1i*kx*Upp+(1/Re)*(KD).^2;
Lsq = 1i*kx*U + (1/Re)*KD;
B = 1i*kz*Up; O = zeros(N,N);

L = [Los O; B Lsq];
M = [KD O; O eye(N)];
L1 = M\L;

%% COMPUTE EIGENVALUES
% Since according to v-omega formulation, the eigenvalues obtained here,
% are related to the frequency as: lambda = i*omega (see derivation)
% lambda = lambdar + i*lambdai --> appears as e^(-lambda*t) in perturbation
% => negative lambdar corresponds to unstable modes
% the most negative lambdar corresponds to the most dangerous perturbation

[shape, lambda] = eig(L1);
lambda = diag(lambda);
omega = lambda/1i;
%% PLOT
% WARNING: Check for v.high values of eigenvalues
% remove them, or change the range of lambda below
v = lambda(100:199);
vr = real(v);
vi = imag(v);

figure
hold on
grid on
sz = size(v);
for i = 1:sz
    scatter(vr(i), vi(i),'xb');
end
title(['Eigenvalues for kx = ' num2str(kx) ', kz = ' num2str(kz)])
xlabel('Real part')
ylabel('Imaginary part')
hold off

y = 0:ymax/100:ymax;
mode = 4;

figure
sgtitle(['f4 (x,$k_x,k_z$) = (' num2str(xl) ',' num2str(kx) ',' num2str(kz) '),
mode = ' num2str(mode)])
```

```
subplot(1,2,1)
hold on
grid on
r = real(shape(1:101,mode));
im = imag(shape(1:101,mode));
plot(r,y)
plot(im,y)
% legend('Real Part', 'Imaginary Part')
title('Eigenfunctions $\hat{v}$')
xlabel('$\hat{v}$')
ylabel('y')
hold off

subplot(1,2,2)
hold on
grid on
r = real(shape(102:202,mode));
im = imag(shape(102:202,mode));
plot(r,y)
plot(im,y)
legend('Real Part', 'Imaginary Part')
title('Eigenfunctions $\hat{\omega}$')
xlabel('$\hat{\omega}$')
ylabel('y')
hold off
```

Spatial Stability using CMM

```
% Initializing velocity(U), angular frequency(w) and mesh size
u = zeros(10,1);
w = zeros(6,1);
w(1) = 1e-8;
w(2) = 1e-1;
for i = 2:9
    w(i + 1) = 10.^(i-1);
end
for i = 1:6
    u(i) = 2.*i;
end
meshsize = [100;1000];
% Calculating alpha for each triplet of u w and meshsize
for i = 1:10
    for j = 1:6
        for k = 1:2
            Rn = 100;
            a_o_guess = -18600;

            [a_o,K1,Re_delta] = test(w(i),u(j),Rn,meshsize(k),a_o_guess);
            if abs(K1)>1
                % this implies that newton raphson has not converged
                Rn = 2.*Rn;
```

```
                [a_o,K1,Re_delta] = test(w(i),u(j),Rn,meshsize(k),a_o_guess);
            end
            if abs(K1)>1
                % this implies newton raphson has failed
                a_o = NaN;
            end
            % Storing alpha and reynolds number
            a(i,j,k) = a_o;
            Re(i,j,k) = Re_delta;
            fprintf('Loop i=%d j=%d k=%d\n',i,j,k);
        end
    end
end
% Plotting
figure
plot(log(w),imag(a(:,1,1)),'--o')
hold on
plot(log(w),imag(a(:,1,2)),'--o')
xlabel('\omega_{o}')
ylabel('Imag(\alpha_{I})')
title(sprintf('Re = %d\n',Re(1,1,1)))
legend('h = 0.1\delta','h = 0.01\delta')

figure
plot(log(w),a(:,2,1),'--o')
hold on
plot(log(w),a(:,2,2),'--o')
xlabel('\omega_{o}')
ylabel('Imag(\alpha_{I})')
title(sprintf('Re = %d\n',Re(1,2,1)))
legend('h = 0.1\delta','h = 0.01\delta')

figure
plot(log(w),a(:,3,1),'--o')
hold on
plot(log(w),a(:,3,2),'--o')
xlabel('\omega_{o}')
ylabel('Imag(\alpha_{I})')
title(sprintf('Re = %d\n',Re(1,3,1)))
legend('h = 0.1\delta','h = 0.01\delta')

figure
plot(log(w),a(:,4,1),'--o')
hold on
plot(log(w),a(:,4,2),'--o')
xlabel('\omega_{o}')
ylabel('Imag(\alpha_{I})')
title(sprintf('Re = %d\n',Re(1,4,1)))
legend('h = 0.1\delta','h = 0.01\delta')

figure
```

```
plot(log(w),a(:,5,1),'--o')
hold on
plot(log(w),a(:,5,2),'--o')
xlabel('\omega_{o}')
ylabel('Imag(\alpha_{I})')
title(sprintf('Re = %d\n',Re(1,5,1)))
legend('h = 0.1\delta','h = 0.01\delta')

figure
plot(log(w),a(:,6,1),'--o')
hold on
plot(log(w),a(:,6,2),'--o')
xlabel('\omega_{o}')
ylabel('Imag(\alpha_{I})')
title(sprintf('Re = %d\n',Re(1,6,1)))
legend('h = 0.1\delta','h = 0.01\delta')

figure
plot(log(w),a(:,1,2),'--o')
hold on
plot(log(w),a(:,6,2),'--o')
xlabel('\omega_{o}')
ylabel('Imag(\alpha_{I})')
title(sprintf('Re = %d\n',Re(1,1,1)))
legend('Re = 496','Re = 1217')


%% This function takes in the angular frequency(w) , the freestream
velocity(_inf)
% and the number of iterations of newton raphson(Rn) , meshsize and the initial
% guess of alpha(a_o_guess) and returns the value of alpha , the value of
% residual for newton raphson(K1), Reynolds number(Re_delta)
function [a_o,K1,Re_delta] = test(w,U_inf,Rn,meshsize,a_o_guess)
syms a y
x = 0.5;
rho = 1.2886;
% U_inf = 50;
mu = 1.83463e-05;
Re_x = rho*U_inf*x/mu;
delta = 5.*x./sqrt(Re_x);
eta =@(y) y./delta;
lambda = 0;
u =@(y) (y>0&y<delta).*U_inf.*(1.5.*eta(y) - 0.5.*(eta(y).^3)) + ...
               lambda.*(eta(y) - 2.*(eta(y).^2) + eta(y).^3)...
               + (y>=delta).*U_inf;
delta_star = integral(@(y) (1 - u(y)/U_inf),0,delta);
% Reynolds_number
Re_delta = rho*U_inf*delta_star/mu;

y1 = linspace(delta.*10,0,meshsize);
% Step-size
```

```
h = delta.*10./(meshsize-1);

Q = sqrt((a.^2) + 1i.*a.*Re_delta.*(1 - (w/a)));
% Initial values
T = [1;-(a + Q);(a.^2) + (a.*Q) + (Q.^2); a.*Q; -a.*Q.*(a + Q);...
      (a.^2).*(Q.^2)];
Q1 = eye(6);
U = u(y1);
U = U./5;%Non-dimensionalizing the velocity field
for i = 1:meshsize
    if i == meshsize
        dU(i) = -(U(i) - U(i - 1))/h;
    else
        dU(i) = -(U(i + 1) - U(i))/h;
    end
end

for i = 1:meshsize
    if i == meshsize
        ddU(i) = -(dU(i) - dU(i - 1))/h;
    else
        ddU(i) = -(dU(i + 1) - dU(i))/h;
    end
end

% loop over all steps

for i = 1:(length(y1)-1)
    h = -h;
    A = A_matrix(a,Re_delta,U(i),ddU(i),w);
    P = eye(6) + A.*h + ((A.*h)^2)./2 + ((A.*h)^3)./6 + ...
        ((A.*h)^4)./24 + ((A.*h)^5)./120;
    T1 = P*Q1;
    Q1 = P;
end
K = T1*T; %getting y1 out of Y
L = K(1);
dL = diff(L,a);

a_o = a_o_guess;
for i = 1:Rn
    K1 = subs(L,a,a_o);
    dK1 = subs(dL,a,a_o);
    a_o = vpa(a_o - K1./dK1);
end

end

%% This function takes in alpha(a) as a symbol
% Reynolds number(Re) the velocity (U) and its double derivative
% and returns the A_matrix
```

```
function A = A_matrix(a,Re,U,ddU,w)
% syms a
c = w./a;
b1 = (2.*a) + 1i.*Re.*a.*(U - c);
b2 = (a.^4) + 1i.*(a.^3).*Re.*(U - c) + 1i.*a.*Re.*ddU;
A = [0 1 0 0 0 0;...
     0 0 1 1 0 0;...
     0 b1 0 0 1 0;...
     0 0 0 0 1 0;...
     b2 0 0 b1 0 1;...
     0 b2 0 0 0 0];
end
```

Model ODE: Simple Harmonic Oscillator

```
[x,u,o] = Model(15);
figure
hold on
xlabel('x')
ylabel('u')
plot(x,u)
hold off

function [x,u,w]=Model(Omega)
% MODEL solves equation:
% u''+omega(x)^2*u=cos(Omega*x),
% where omega(x)=pi+x/2.
xlims = [0 25];
y0 = [0;0];
[x,Y] = ode45(@(x,y) fcn(x,y,Omega),xlims,y0);

u = Y(:,1);
w=omega(x);

    function dy = fcn(x,y,Omega)
        dy=[y(2); cos(Omega*x)-omega(x).^2.*y(1)];
    end
    function w=omega(x)
        w=pi+x/2;
    end
end
```

Bromwich Integral

```
syms a y x t
y = 0.002;
w0 = 0.1;
a_i = -0.02;
Re_delta = 1196;
Q = sqrt((a.^2) + 1i.*a.*Re_delta.*(1 - (w0./a)));
```

```
phi_1 = exp(-a.*y);
dphi_1 = -a.*exp(-a.*y);
phi_3 = exp(-Q.*y);
dphi_3 = -Q.*exp(-Q.*y);
psi = (phi_1.*subs(dphi_3,y,0) - phi_3.*subs(dphi_1,y,0))./...
      (subs(phi_1,y,0).*subs(dphi_3,y,0) - subs(phi_3,y,0).*subs(dphi_1,y,0));
psi = psi.*exp(1i.*(a.*x - w0.*t));
K = @(x) int(psi(x), a, -20-(0.02*1i), 20-(0.02*1i));
X = linspace(-20,100,121);
plot(X,imag(K(X)))
```

Links to the presentations:

[P1: Literature Review]

[P2: Base Flow and Stability Analysis]

[P3: Receptivity Analysis]

7. References

1. Antar, B.N., & Benek, J.A. (1978). *Temporal eigenvalue spectrum of the Orr–Sommerfeld equation for the Blasius boundary layer*. Physics of Fluids (1958-1988) 21, 183 (1978) doi: 10.1063/1.862212
2. Charru, F. (2011). *Hydrodynamic Instabilities* (Cambridge Texts in Applied Mathematics) (P.De Forcrand-Millard, Trans.). Cambridge: Cambridge University Press. doi:10.1017/CBO9780511975172
3. Friedrich, R. (1999). *Modelling of turbulence in compressible flows*. In Transition, Turbulence and Combustion Modelling, ERCOFTAC Series vol 6 Edited by: Hanifi, A.Reshotko, Eli. (2003).
4. *Boundary-Layer Stability and Transition*. Ann. Rev. Fluid Mech. 8. 311-349. doi:10.1146/annurev.fl.08.010176.001523
5. Peter G. Baines, Sharan J. Majumdar, and Humio Mitsudera, "The mechanics of the Tollmien-Schlichting wave," *J. Fluid Mech.*, vol. 312, 1996, pp. 107-124.doi:10.1017/S0022112096001930
6. Schlichting, H. & Gersten, K. (2017). *Boundary-Layer Theory*. Springer doi:10.1007/978-3-662-52919-5
7. Schmid, P.J. & Henningson, D.S. (2001). *Stability and Transition in Shear Flows*. Springer doi:10.1007/978-1-4613-0185-1
8. Sengupta, T.K., Ballav, M. & Nijhawan, S. (1994). *Generation of Tollmien–Schlichting waves by harmonic excitation*. Physics of Fluids (1994-present) 6, 1213 (1994); doi: 10.1063/1.868290
9. Sengupta T.K. *Instabilities of Flows and Transition to Turbulence.* CRC Press (2012)
10. Hydrodynamic Instabilities, by François Charru, Cambridge University Press, (2011)
11. Reshotko, Eli. (2003). *Boundary-Layer Stability and Transition*. Ann. Rev. Fluid Mech.. 8. 311-349. 10.1146/annurev.fl.08.010176.001523